Development 133, 3039-3049 (2006) doi:10.1242/dev.02471

Wnt9a signaling is required for joint integrity and regulation of *Ihh* during chondrogenesis

Daniela Später[1], Theo P. Hill[1], Roderick J. O'Sullivan[1], Michaela Gruber[1,*], David A. Conner[2] and Christine Hartmann[1,†]

Joints, which separate skeleton elements, serve as important signaling centers that regulate the growth of adjacent cartilage elements by controlling proliferation and maturation of chondrocytes. Accurate chondrocyte maturation is crucial for endochondral ossification and for the ultimate size of skeletal elements, as premature or delayed maturation results predominantly in shortened elements. Wnt9a has previously been implicated as being a player in joint induction, based on gain-of function experiments in chicken and mouse. We show that loss of *Wnt9a* does not affect joint induction, but results to synovial chondroid metaplasia in some joints. This phenotype can be enhanced by removal of an additional Wnt gene, *Wnt4*, suggesting that Wnts are playing a crucial role in directing bi-potential chondro-synovioprogenitors to become synovial connective tissue, by actively suppressing their chondrogenic potential. Furthermore, we show that Wnt9a is a temporal and spatial regulator of Indian hedgehog (*Ihh*), a central player of skeletogenesis. Loss of Wnt9a activity results in transient downregulation of *Ihh* and reduced Ihh-signaling activity at E12.5-E13.5. The canonical Wnt/β-catenin pathway probably mediates regulation of *Ihh* expression in prehypertrophic chondrocytes by Wnt9a, because embryos double-heterozygous for Wnt9a and β-catenin show reduced *Ihh* expression, and in vivo chromatin immunoprecipitation demonstrates a direct interaction between the β-catenin/Lef1 complex and the *Ihh* promoter.

KEY WORDS: Wnt, Synovial joint, Chondrocyte maturation, Ihh, Mouse

INTRODUCTION

Joints, which separate adjacent skeletal elements from each other, are important signaling centers that control chondrocyte maturation within the opposing skeletal elements (Francis-West et al., 1999). Three different types, synovial (e.g. joints in the limb), fibrous (e.g. sutures in the skull) and cartilaginous (e.g. joints between vertebral bodies) joints can be distinguished. In the limb, the process of joint formation and differentiation of skeletal elements are tightly linked. The limb skeletal elements are formed by endochondral ossification, a process starting with the condensation of mesenchymal cells forming pre-cartilaginous condensations. It has been proposed that the first step in joint formation is to inhibit cells within the prospective joint region from differentiating into chondrocytes, while neighboring cells can take on this fate and contribute to the cartilage elements. Cells within the prospective joint region form the so-called interzone, which is densely packed and contains flattened cells. Joint interzone cells produce different types of collagens, type I and III, compared with chondrocytes, which produce collagen type II (Ralphs and Benjamin, 1994). The interzone also expresses molecules such as Wnt9a (formerly called Wnt14) and the BMP antagonist Noggin, which are implicated in regulating the non-chondrogenic nature of these cells (Brunet et al., 1998; Debeer et al., 2005; Gong et al., 1999; Guo et al., 2004; Hartmann and Tabin, 2001). In addition, the interzone expresses factors such as parathyroid-hormone related peptide (Pthrp; Pthlh – Mouse Genome Informatics), Wnt4, Fgf18, growth differentiation factors (Gdf5, Gdf6 and Gdf7), and various members of the bone morphogenetic proteins (BMPs) that regulate growth and differentiation of the adjacent cartilage elements (Francis-West et al., 1996; Hartmann and Tabin, 2000; Merino et al., 1999; Ohbayashi et al., 2002; Storm et al., 1994; Storm and Kingsley, 1996). Recent data suggest that the diverse cell types present in the mature synovial joints, such as synovial cells, articular permanent chondrocytes and cells of the joint capsule, originate from the interzone region (Archer et al., 2003; Rountree et al., 2004).

The molecular mechanisms underlying joint formation are not yet well understood. Various signaling molecules, such as Gdf5, Gdf6 and Noggin have been implicated in joint formation (Brunet et al., 1998; Settle et al., 2003; Storm and Kingsley, 1996). However, none of those factors is sufficient to induce joint formation (Capdevila and Johnson, 1998; Merino et al., 1999; Pathi et al., 1999; Pizette and Niswander, 2000; Storm and Kingsley, 1999; Tsumaki et al., 2002). By contrast, disruption of integrin signaling and ectopic activation of Wnt9a signaling leads to the induction of molecular markers characteristic for the joint-interzone and the formation of joint-like regions (Garciadiego-Cazares et al., 2004; Guo et al., 2004; Hartmann and Tabin, 2001). Based on this, it has been proposed, that Wnt9a signaling is involved in joint induction.

Factors secreted by cells adjacent to the joint, such as Pthrp, Fgf18 and others, are important regulators for the maturation of chondrocytes, from proliferative, to postmitotic prehypertrophic, to hypertrophic chondrocytes, which mature further and eventually undergo apoptosis. Accurate control of chondrocyte proliferation and maturation is crucial for determining the future size of the skeletal element. A key regulator for these processes is the signaling molecule *Ihh*, which is produced by prehypertrophic/early hypertrophic chondrocytes and plays essential roles in skeletogenesis coordinating cartilage growth and osteoblastogenesis: Ihh signaling controls the expression of another secreted molecule, Pthrp, that negatively regulates chondrocyte

[1]Institute of Molecular Pathology, Dr Bohr-Gasse 7, A-1030 Vienna, Austria.
[2]Department of Genetics, Harvard Medical School, 77 Avenue Louis Pasteur, Boston, MA 02115, USA.

*Present address: Department of Cell and Developmental Biology, University of Pennsylvania Cancer Center, 421 Curie Boulevard, Philadelphia, PA19104,USA
†Author for correspondence (e-mail: hartmann@imp.univie.ac.at)

Accepted 2 June 2006

maturation. Furthermore, Ihh has additional Pthrp-independent roles; it stimulates chondrocyte proliferation and osteoblast differentiation (Kronenberg, 2003). *Ihh* expression is under transcriptional control by *Runx2* and *Runx3* (Yoshida et al., 2004), and it expression levels are regulated in an antagonistic manner by Fgf and Bmp signaling (Minina et al., 2002). Modulation in the expression of secreted factors controlling the central regulator Ihh affect growth and differentiation of the skeletal elements, resulting primarily in a shortening of the skeletal elements.

In order to address whether *Wnt9a* is necessary for joint induction, we have targeted the *Wnt9a* locus and generated two alleles, a conditional allele and a *lacZ* knock-in allele. *Wnt9a* loss-of-function mutants die at birth. They display partial joint fusions of carpal and tarsal elements and chondroid metaplasia in synovial and fibrous joints. The phenotypes associated with synovial joints are augmented in *Wnt9a;Wnt4* double mutants. Our data demonstrate that Wnts are essential to maintain joint integrity, but that they are probably not required for inducing joint formation. In addition, we found that *Wnt9a* mutants have shortened appendicular long bones. The shortening is due to a temporary downregulation of *Ihh* expression in *Wnt9a* mutants at embryonic days E12.5-13.5. Furthermore, we show by genetic interaction and by in vivo chromatin immunoprecipitation that the regulation of *Ihh* expression and chondrocyte maturation by Wnt9a is mediated through β-catenin.

MATERIALS AND METHODS

Generation of Wnt9a mutant alleles

The targeting construct of the conditional Wnt9a allele was generated as follows: a FRT-flanked neomycin resistance gene (neo) driven by the PGK promoter with an 3′ located loxP site (Sun et al., 2000) was inserted into an *Spe*I restriction site 357 bp upstream of exon 2. A double-stranded loxP oligo was ligated into an ApaLI site 67 bp downstream of exon 2. The *lacZ* targeting construct was generated by introducing an SA-IRES-*lacZ*-SV40pA-FRT-*PGK-neo*-FRT cassette into the *Sma*I site of exon 2. Positively targeted ES cells were identified by Southern blot analyses using external 5′ and 3′ probes on *Eco*RV-digested genomic DNA (frequency: 1 in 25 in the C1 ES cell line) and introduced into mouse blastocysts (Hendrickson et al., 1995). Four independently targeted ES-cell clones were used to generate chimeras (two for each allele), three of which transmitted the recombinant alleles (only one for the conditional allele). Exon 2 was deleted in the germline using Prx1Cre females. Genotyping was performed by PCR (primer sequences available upon request). Phenotypes for embryos homozygous for either of the two *Wnt9a* alleles (Δ or *lacZ*) were identical on mixed, random bred (Swiss-Webster), F1 (129/Sv; C57Bl6/J) and inbred (129/Sv) backgrounds.

Mouse strains

Wnt4 heterozygous mice were purchased from Jackson laboratory. Genotyping of *Wnt4* and β-catenin alleles (lacZ and floxed) was performed by PCR as previously described (Huelsken et al., 2000; Huelsken et al., 2001; Stark et al., 1994). Limbs lacking β-catenin activity in the mesenchyme were generated as described by Hill et al. (Hill et al., 2005).

Skeletal analysis

Newborn pups (P0) and embryos were skinned, eviscerated and fixed in 95% ethanol. Alizarin Red/Alcian Blue or Alcian Blue staining of the skeletons were performed as described previously (McLeod, 1980).

β-Galactosidase staining, histology, in situ hybridization and BrdU incorporation

For β-galactosidase staining, embryos E9.5-E13.5 were fixed for 15-30 minutes and skinned newborns were fixed for 1 hour in 0.1 M phosphate buffer containing 0.2% glutaraldehyde, 2 mM Mg_2Cl, 5 mM EGTA on ice, washed three times in 0.1 M phosphate buffer containing 0.01% deoxycholate. 0.02% NP-40 and 2 mM Mg_2Cl at room temperature, and stained overnight at 37°C in staining solution [1 mg/ml X-gal, 4% diethyl formamide, 5 mM $K_3(Fe(CN)_6)$, 5 mM $K_4(Fe(CN)_6)$].

For histology and section in situ hybridization, tissue was treated as previously described (Hill et al., 2005). For analysis of BrdU incorporation, 50 μg BrdU/g body weight was injected intra-peritoneally into pregnant mice 2 hours before sacrifice. BrdU incorporation was detected on sections by immunohistochemistry (Zymed Laboratories). For each analysis and developmental stage, at least three independent samples were analyzed.

RT-PCR analysis

For RT-PCR and real-time PCR analysis, 1 μg total RNA was used to produce first-strand cDNA. Real-time PCR was performed by using SYBR green 1 nucleic acid gel stain (Molecular Probes) and TAKARA Taq. Values were calculated using the comparative C(t) method and normalized to mouse *Hprt1* expression. Primer sets were tested by dilution series and products were analyzed by gel electrophoresis and melting curves. All primer sequences are available by request.

Retroviral work and cultivation of chondrocytes

The RCAS-AP, RCAS-Wnt5a, RCAS-Wnt9a, RCAS-Wnt3a and RCAS-caβ-cat viruses has been previously described (Hartmann and Tabin, 2000; Hartmann and Tabin, 2001; Kengaku et al., 1998). Chondrocytes isolated from the caudal part of day 18 chick sternae (Koyama et al., 1999) were cultured for 1 day, collected and plated at a density of 5×10^5 cells/well in a six-well plate. The following day chondrocytes were infected using 5 μl viral supernatant per well (titers: $6\text{-}8\times10^8$ pfu/ml) and cultured for 3-4 days in DMEM:F12 (Invitrogen). Experiments were carried out in triplicate.

Western blot analysis

For Western blot analysis, protein was extracted from cultured chicken sternal chondrocytes infected with different RCAS viruses. Extracts of 50 μg per lane were loaded. Luminal detection was performed using an antibody against chicken β-catenin (1:800, Sigma C7027), followed by incubation with a HRP-conjugated secondary antibody (1:2500; Promega).

Limb explant cultures

Forelimbs were skinned and removed from E12.5 and E13.5 embryos. One limb of a forelimb pair was cultured in the presence of 25 μM SU5402 (Calbiochem)/0.2% DMS0, while the other one was cultured in 0.2% DMSO in DMEM:F12 (Invitrogen) supplemented with 10% FCS and L-Glutamine. Limbs were cultured for 24 hours in 24-well dishes floating on top of Nuclepore Track-Etch Membranes (Whatman) in a humidified tissue culture incubator at 37°C and 5% CO_2.

Immunohistochemical staining

For immunohistochemical staining of cultured caudal chondrocytes, cells were fixed for 15 minutes at room temperature with 4% paraformaldehyde in PBS, washed twice with PBS. Endogenous peroxidase activity was inactivated by incubating the cells for 30 minutes in 1% H_2O_2 in PBS. Cells were subsequently washed three times with PBS; blocked for 30 minutes with PBS, 10% FCS and 0.1% Triton-X100; and incubated with the primary antibodies against collagen type II (II-II6B3 supernatant, 1:30) and collagen type III (3B2 supernatant 1:30) from the Developmental Hybridoma Bank (Iowa). The signal was detected using a biotinylated anti-mouse secondary antibody (dilution 1 in 250; Vector Laboratories) in combination with the ABC kit (Vector labs) and DAB (Sigma) as a substrate. β-Catenin immunohistochemical staining on paraffin sections was performed using the anti-β-catenin (BD Transduction Laboratories, 1 in 250) after heat-induced citrate buffer antigene retrieval. Signal detection was performed as described above.

Chromatin immunoprecipitation (ChIP)

For in vivo cartilage lysates, humeri were dissected from 13.5 dpc limbs (FVBN mice: litters with 10-13 embryos). Humeri of one litter were dissociated in 500 μl of 0.3% collagenase IV/0.1% Trypsin/2% FCS/DMEM for 15 minutes at 37°C and by additional usage of a bouncer. After a PBS wash, cells were crosslinked with 1% formaldehyde for 10 minutes, followed by quenching with 125 mM glycine. Whole-cell extracts were prepared for ChIP as described (Martens et al., 2005). Approximately

200 μg of fragmented chromatin was used in immunoprecipitation with 4 μg β-catenin (St. Cruz, sc-1496), 4 μg Lef1 (St. Cruz, sc-8592) and 4 μg H3-K4 methylation (Upstate Biotechnology) antibodies. Purified DNA from immunoprecipitates, as well as of the input material was analyzed by real-time PCR using the Roche Sybr green quantitation method on a MJ research Lightcycler (*n*=3). Results were normalized and presented as percentage of input DNA. For amplification of the three potential TCF/LEF1 sites, the following primer pairs were used: site 1 forward, 5′ TCCGGCTGCGACGTGGGTTGC 3′; site 1 reverse, 5′ CGGCCGGCG-GACTGAAGG 3′; site 2 forward, 5′ ACTCCCCTGCCATC-CCAGCACTCC 3′; site 2 reverse, 5′ GACGGGCACTGCCTGGGAAT-CACT 3′; site 3 forward, 5′ TGAATCCCGAGCAAGGCGTAG 3′; site 3 reverse, 5′ TGGGATGGCAGGGGAGTAGTA 3′.

RESULTS

Generation of Wnt9a mutant alleles

Two *Wnt9a* alleles were generated by targeting the genomic *Wnt9a* locus in embryonic stem cells: a conditional allele with loxP sites flanking exon 2 (Fig. 1A) and a lacZ-knock-in allele with an IRES-lacZ-FRT-neo cassette inserted into exon 2 (Fig. 1A). Germline transmission and proper targeting of mutant alleles was verified by Southern blot (Fig. 1B). Mice heterozygous for the deleted (Δ) allele were obtained by germline deletion of the floxed exon 2 (Fig. 1B). A truncated transcript, resulting from aberrant splicing of exon 1 to exon 3, could be amplified by RT-PCR from RNA of $Wnt9a^{\Delta/\Delta}$ mutant embryos (Fig. 1C). Sequencing revealed a frame-shift and a premature Stop. Any protein made from this transcript would therefore consist of 65 amino acids, containing the first 32 amino acids of the Wnt9a protein. In the *lacZ* allele, the open reading frame of *Wnt9a* was disrupted and thus no functional protein can be translated from this allele. We consider both alleles as being null alleles and therefore we will refer to them as –allele, unless otherwise noted. No pups homozygous for either of the mutant alleles were recovered at weaning from heterozygous intercrosses of $Wnt9a^{+/\Delta}$ or $Wnt9a^{+/lacZ}$ mice. Homozygous mutant pups died within 12 hours of birth, for so far unknown reasons. Histological analyses of their major organs, heart, lung, liver, intestinal tract, kidney and brain, did not reveal any obvious abnormalities. They are slightly smaller than their littermates and can be readily identified by the absence of milk in their stomach (Fig. 1D).

Homozygous Wnt9a mutants display skeletal abnormalities

Comparative skeletal analyses of $Wnt9a^{-/-}$ newborns with their heterozygous and wild-type littermates revealed no gross joint defects but a number of skeletal abnormalities (Fig. 2A and data not shown). In all of the *Wnt9a* mutants, there was an ectopic Alcian Blue-positive nodule present in the elbow region (Fig. 2A, Fig. 3A, part a′). In addition, the appendicular long bones were slightly reduced in length and showed an even greater reduction in the size of the mineralized regions (Fig. 2A). These reductions were more prominent in the proximal bones, such as scapula and humerus, and ileum and femur (Fig. 2B; data not shown). The hyoid bone and atlas were hypoplastic (Fig. 2A). In the skull, the supraoccipital bone showed reduced mineralization and the frontal bones were further apart (Fig. 2C, part a). The basioccipital bone was abnormally shaped and reduced in size (Fig. 2C, part b). Furthermore, the cartilaginous base was extended dorsally, particularly noticeable at the base of the parietal bones (Fig. 2C, part c,e-f′). In addition ectopic cartilage nodules were present within the midline sutures (Fig. 2C, part d-f′).

Chondroid metaplasia of fibrous and synovial joint cells in Wnt9a mutants

$Wnt9a^{-/-}$ newborns display no obvious defects with respect to fusions of major joints. However, ectopic cartilaginous material was detected by Alcian Blue staining in the interfrontal and sagittal

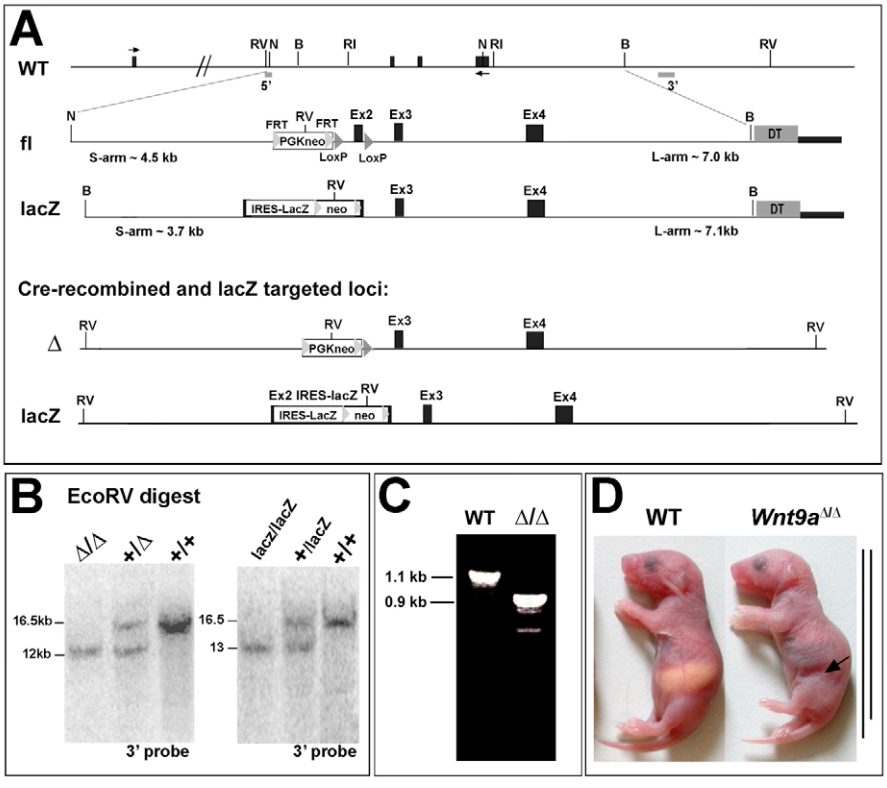

Fig. 1. Construction of Wnt9a alleles and analysis of mutants. (**A**) Schematic of the two targeting constructs, which were introduced into the Wnt9a locus on mouse chromosome 11. Floxed allele (fl): exon 2 (Ex2) flanked by loxP sites. *lacZ* allele: insertion of an IRES-lacZ cassette into exon 2. The 5′ and 3′ external probes are indicated below the genomic locus map. Restriction enzymes: B, *Bam*HI; N, *Nhe*I; RI, *Eco*RI; RV, *Eco*RV. (**B**) Southern-blot on *Eco*RV-digested genomic DNA from mutant (Δ/Δ or lacZ/lacZ), heterozygous (+/Δ or +/lacZ) and wild-type (+/+) E10.5 littermates from intercrosses of +/Δ and +/lacZ heterozygous mice, respectively, hybridized with the 3′ genomic external probe. (**C**) RT-PCR using RNA obtained from E10.5 wild-type and $Wnt9a^{\Delta/\Delta}$ embryos, showing the presence of a 1.1 kb transcript in wild type and a shorter 900 bp transcript in $Wnt9a^{\Delta/\Delta}$ mutants. (**D**) Wild-type (WT) and $Wnt9a^{\Delta/\Delta}$ mutant newborn littermates. Mutants are slightly smaller (indicated by the shorter black line on the right side) and that they do not have milk in the stomach (arrow).

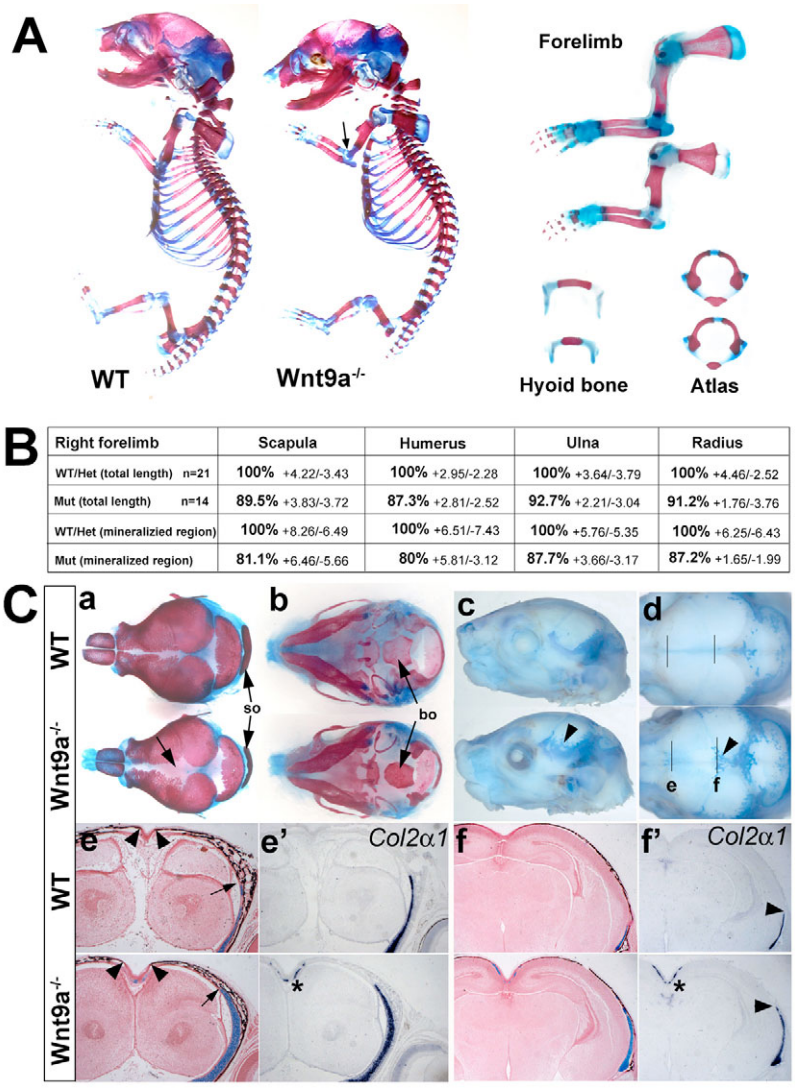

Right forelimb	Scapula	Humerus	Ulna	Radius
WT/Het (total length) n=21	100% +4.22/-3.43	100% +2.95/-2.28	100% +3.64/-3.79	100% +4.46/-2.52
Mut (total length) n=14	89.5% +3.83/-3.72	87.3% +2.81/-2.52	92.7% +2.21/-3.04	91.2% +1.76/-3.76
WT/Het (mineralizied region)	100% +8.26/-6.49	100% +6.51/-7.43	100% +5.76/-5.35	100% +6.25/-6.43
Mut (mineralized region)	81.1% +6.46/-5.66	80% +5.81/-3.12	87.7% +3.66/-3.17	87.2% +1.65/-1.99

Fig. 2. Skeletal abnormalities in *Wnt9a* mutants. (**A**) Alizarin Red/Alcian Blue staining of skeletons of wild-type and *Wnt9a*$^{-/-}$ E17.5 littermates, and of forelimbs, hyoid bones, atlas from WT (on top) and *Wnt9a*$^{-/-}$ (below) newborn littermates. Smaller mineralized zones are found in the scapula and humerus, and, to a lesser extend, in ulna and radius in the mutant forelimbs compared with wild type. Hypoplastic hyoid bone and atlas. (**B**) Table showing quantification of size reduction with regard to the total length and the mineralized regions of mutant skeletal forelimb elements (Mut=*Wnt9a*$^{lacZ/lacZ}$) in comparison with those from wild type (wild type=*Wnt9a*$^{+/+}$) and heterozygous (Het=*Wnt9a*$^{+/lacZ}$). Average length of wild-type/heterozygous elements was set to 100%. Mutant and littermate control limbs were collected from seven litters. (**C**) Dorsal (a) and ventral (b) view of Alizarin Red/Alcian Blue-stained wild-type and *Wnt9a*$^{-/-}$ heads from newborns, showing that in *Wnt9a*$^{-/-}$ the frontal bones are further apart (arrow in a), a smaller ossification center in the supraoccipital (so) bone and an abnormally shaped basioccipital bone (bo) (arrow in b). (c) Lateral and (d) dorsal view of Alcian Blue-stained wild-type and *Wnt9a*$^{-/-}$ newborn heads, showing expansion of the cartilaginous base in the region of the parietal bone (arrowhead in c) and presence of ectopic Alcian Blue-positive areas in the sagittal suture of the skull (arrowhead in d). (e,f) Coronal sections through skulls of wild-type and *Wnt9a*$^{-/-}$ newborns, at the levels indicated in d. Van Kossa/Alcian Blue-stained sections (e,f), showing that the two frontal bone plates are further apart from each other in *Wnt9a* mutants (arrowheads in e), dorsal expansion of the cartilaginous base (arrow) and the presence of Alcian Blue-positive cells in the sagittal suture region of the *Wnt9a* mutant skull. (e′,f′) *Col2a1* in situ hybridization on sections adjacent to those shown in e,f, showing *Col2a1*-expressing cells within the sagittal suture (asterisks), which are absent in the wild-type littermates.

suture regions, separating frontal and parietal bones, respectively (Fig. 2C, parts d,e′,f′; data not shown) and in the elbow joint (Fig. 3). Sutures are fibrous joints between the flat bones of the cranial vault, which serve as major sites for bone expansion during postnatal skull growth (Opperman, 2000). Van Kossa staining showed that the mineralized regions were further apart in mutant than wild-type skulls (Fig. 2C, part e). In situ hybridization of coronal skull sections revealed that the chondrocyte markers *Col2a1* and *Sox9* were ectopically expressed in cells within the frontal and sagittal sutures (Fig. 2C, parts e′,f′; data not shown). In addition, their normal expression domains at the base were expanded dorsally (Fig. 2C, parts f,f′).

An ectopic Alcian Blue-stained nodule was observed in the humeral-radial space of all *Wnt9a* mutant newborns (n=24; Fig. 3A, part a′). Histological analyses on sections of P0 *Wnt9a*$^{-/-}$ forelimbs revealed that cells within the synovial fold had a chondrocyte-like appearance (Fig. 3A, part b′) and expressed *Sox9* and *Col2a1* (Fig. 3A, part c′; data not shown). In humans, this phenotype of synovial cells differentiating into chondrocytes forming loose ectopic cartilaginous nodules is referred to as synovial chondroid metaplasia or synovial chondromatosis. The onset of synovial chondroid metaplasia in the humeral-radial joint (HRJ) of *Wnt9a* mutants was detectable as early as E15.5 by in situ hybridization [showing expression of the chondrogenic marker *Sox9* in a broad domain within the HRJ region (Fig. 3A, part d′)], while *Col2a1* expression was restricted to a few cells within this region (Fig. 3A, part e′). Additional joint abnormalities were observed in *Wnt9a* mutants, such as partial joint fusions between the navicular and intermediate cuneiform tarsal elements in the foot and between the carpal elements c and 3 in the wrist (Fig. 3A, parts f′,g′). These data suggest that Wnt9a signaling is required in some joints to maintain the identity of joint cells.

Wnt9a misexpression in chondrocytes leads to dedifferentiation associated with stabilization of β-catenin

Loss of *Wnt9a* signaling in HRJ and midline suture cells led to their ectopic differentiation into chondrocytes. Based on this, we hypothesized that Wnt9a signaling in synovial and fibrous joint cells is required to suppress their chondrogenic potential. To test this hypothesis further, we asked whether ectopic *Wnt9a* signaling in chondrocytes would lead to alterations of the cells. We used primary chicken sternal chondrocytes and infected them with replication competent avian retroviruses (RCAS) expressing either Wnt9a, the canonical ligand Wnt3a, the non-canonical ligand Wnt5a, a constitutively active form of β-catenin (caβ-cat) or alkaline

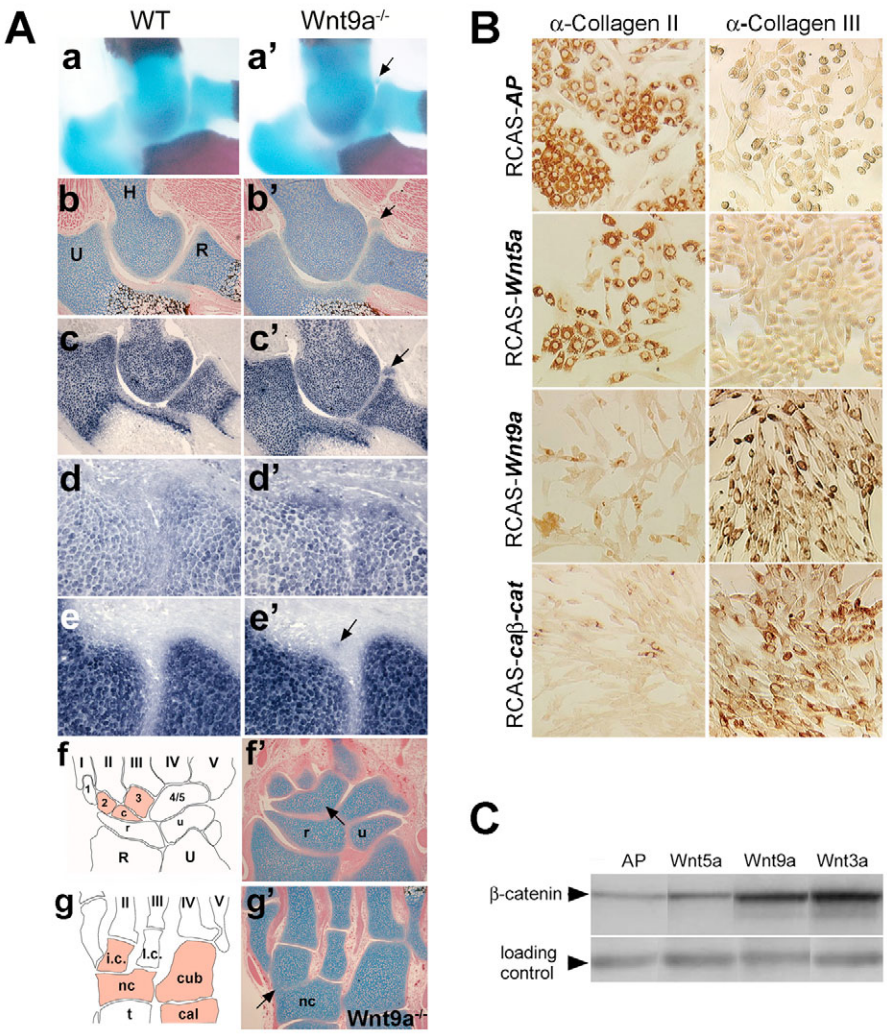

Fig. 3. Loss of Wnt9a leads to defects in joints, and ectopic Wnt9a can transform chondrocytes in fibroblast-like cells. (**A**) P0 forelimbs stained with Alcian Blue/Alizarin Red. (a) Wild-type elbow region; (a′) *Wnt9a*$^{-/-}$ elbow, in which an ectopic Alcian Blue-stained nodule is present in the humeral-radial joint (HRJ) (arrow). Serial sections of wild-type (b,c) and *Wnt9a*$^{-/-}$ (b′,c′) P0 forelimbs, showing Alcian Blue (arrow in b′) and *Col2a1*-positive (arrow in c′) chondrocytes instead of synovial cells within the HRJ fold. Serial sections of wild-type (d,e) and *Wnt9a*$^{-/-}$ (d′,e′) at E15.5, showing that in the mutant cells in the HRJ region express *Sox9* (d′), and that a small cluster of cells expresses *Col2a1* (arrow in e′). (f) Schematic diagram of the carpal elements, metacarpal elements of digits I-V and distal row of carpal elements 1-5 in wild type. c, central carpal element; r and u, radial and ulnar element; R and U, radius and ulna. (f′) Partial fusion between carpal elements c and 3 (arrow) in *Wnt9a*$^{-/-}$. (g) Schematic diagram of the tarsal elements in wild type; Cal, calcaneus; cub, cuboid; l.c., lateral cuneiform; i.c., intermediate cuneiform; nc, navicular; t, tarsal; metatarsal elements of digits II-V. (g′) Partial joint fusion between the intermediate cuneiform and navicular tarsal elements (arrow) in the mutant. (**B**) Immunohistochemical staining for collagen type II and collagen type III on chicken sternal chondrocytes infected with RCAS-AP, RCAS-Wnt5a, RCAS-Wnt9a and RCAS-caβ-cat, showing that Wnt9a and caβ-cat-infected chondrocytes change their morphology, and that instead of producing collagen type II they synthesize collagen type III. (**C**) Western blot for β-catenin using protein extracts from infected chondrocytes, showing that cells infected with a RCAS virus expressing Wnt9a or Wnt3a have increased β-catenin levels.

phosphatase (AP) as control. In AP and Wnt5a-infected cultures, the chondrocytes retained their typical cuboidal shape and stained positive for collagen type II (Col2; Fig. 3B). By contrast, cells infected with either Wnt9a, Wnt3a or caβ-cat viruses had a fibroblastic appearance and ceased to produce Col2 (Fig. 3B, and data not shown). These cells stained positively for collagen type III (Col3) instead, which was not produced by the control cells (Fig. 3B). Western blots from whole-cell extracts revealed that the β-catenin levels were increased in chondrocytes infected with Wnt9a or Wnt3a virus compared with AP or Wnt5a-infected cell extracts (Fig. 3C).

These data show that gain of Wnt9a signaling leads to increased β-catenin levels, and that this increase can transform chondrocytes into fibroblast-like cells producing a different type of collagen.

Wnt4 and Wnt9a act cooperatively in maintaining joint integrity

Surprisingly, only a few synovial joints were affected in *Wnt9a* mutants, despite the fact that *Wnt9a* is expressed in all joints (see Fig. S1 in the supplementary material). At least two other Wnt genes, *Wnt4* and *Wnt16*, are expressed in joints (Guo et al., 2004; Hartmann and Tabin, 2000; Hartmann and Tabin, 2001). *Wnt4* mutants do not have any joint abnormalities (Stark et al., 1994). However, mice double mutant for *Wnt9a* and *Wnt4* (*Wnt9a*$^{-/-}$;*Wnt4*$^{-/-}$) developed synovial chondroid metaplasia in two additional major joints, the ankle and knee joint (n=4; Fig. 4A, parts d,e). In addition, fusions of tarsal and carpal elements were observed in the foot (calcaneus and cuboid, and navicular and intermediate cuneiform) (Fig. 4A, parts f,g) and wrist (carpal elements 2, c and 3) (n=4/4; Fig. 4B, part e). In one specimen, we observed the presence of an ectopic cartilage piece in a ligament (see asterisk in Fig. 4A, part g).

In order to address whether joint formation or maintenance were affected by the loss of *Wnt9a* and *Wnt4*, we analyzed the expression of various markers *Col2a1*, *Col3*, *Gdf5*, *Gli3* and *Wnt4* in E13.5 and E15.5 wrists, focusing primarily at the carpal elements 2, c and 3. Those can be distinguished as separate elements in wild-type and mutant wrists at E13.5, showing identical marker expression (Fig. 4B, parts b,f; data not shown). However, at E15.5 the elements were fused and joint marker expression was lost (Fig. 4B, parts g,h). These observations strongly suggest that the joints are originally formed and that the fusion of skeletal elements occurs secondarily, owing to the absence of Wnt9a and Wnt4 activity.

Altered chondrocyte maturation in Wnt9a mutants

The reduction of the mineralization/ossification centers in skeletal elements formed by endochondral ossification (Fig. 2A,B) suggested a possible delay of chondrocyte maturation in *Wnt9a*

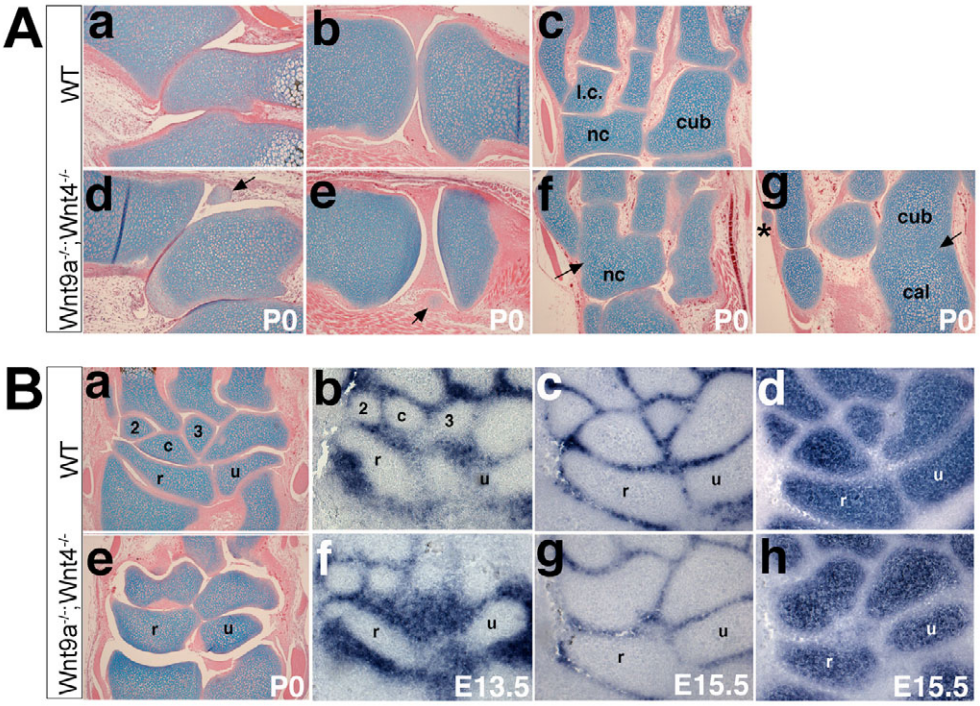

Fig. 4. *Wnt9a* and *Wnt4* act redundantly in maintaining joint integrity. (**A**) Van Kossa/Alcian Blue/Eosin-stained sections through the ankle (a,d), knee (b,e) and foot region (c,f,g) of wild-type (=*Wnt9a*$^{+/-}$; *Wnt4*$^{+/-}$) and *Wnt9a*$^{-/-}$;*Wnt4*$^{-/-}$ newborn littermates. (a) Ankle joint. (b) Knee joint. (c) Foot region. (d,e) Synovial chondroid metaplasia in the ankle joint (d, arrow) and in the joint capsule of the knee (e, arrow) of *Wnt9a*$^{-/-}$;*Wnt4*$^{-/-}$ mutants. (f) Fusion between the intermediate cuneiform and navicular tarsal elements (arrow). (g) Fusion between the calcaneus and cuboid tarsal elements (arrow) and synovial chondroid metaplasia in the joint capsule ligament of digit I (asterisk). (**B**) Sections through the wrist regions of newborns, E13.5 and E15.5 embryos. (a,e) Van Kossa/Alcian Blue/Eosin staining, showing normal arrangement of carpal elements in wild type (a) and fusion of the three carpal elements 2, c and 3 in *Wnt9a*$^{-/-}$;*Wnt4*$^{-/-}$ mutants (e). (b,f) *Gdf5* staining on wrist sections. The three carpal elements 2, c and 3 are separated in wild type (b) and *Wnt9a*$^{-/-}$;*Wnt4*$^{-/-}$ mutants at E13.5 (f). (c,g) *Gdf5* staining on wrist sections. The three carpal elements are separated in wild type (d) but are fused in the *Wnt9a*$^{-/-}$;*Wnt4*$^{-/-}$ mutants (g). (d,h) *Col2a1* staining. The carpal elements in wild type (d) but are fused in *Wnt9a*$^{-/-}$;*Wnt4*$^{-/-}$ mutants (h).

mutants. In order to determine the nature and onset, we performed histological and molecular marker analyses on the developing long bones at different embryonic stages. Whole-mount and section in situ analyses at E11.5 using the early chondrogenic markers *Sox9* and *Col2a1* revealed no difference in the overall size of the long bone anlagen between *Wnt9a* mutants and littermate controls (data not shown). Proliferation rate (BrdU) and apoptosis (TUNEL) were also not altered (data not shown). Furthermore, the chondrocyte differentiation marker *Ihh* was expressed in *Wnt9a* mutant humeri in a domain of similar size and at levels equal to those detected in wild-type or heterozygous littermates (Fig. 5A; data not shown). At E12.5, however, *Ihh* expression levels were slightly downregulated in mutants (Fig. 5B) and this downregulation was even more pronounced at E13.5 (Fig. 5C). Downregulation of *Ihh* was independently confirmed by real-time PCR analysis on cDNA generated from E12.5 and E13.5 wild-type and mutant humeri (see Fig. S2A in the supplementary material).

Surprisingly, at E14.5 *Ihh* expression levels were similar to those in wild-type humeri. Nevertheless, the *Ihh* domain was not yet separated by a population of more mature, *Ihh*-negative chondrocytes (Fig. 5D) and resembled wild-type expression at E13.5 (compare Fig. 5D with Fig. 6C). Temporary downregulation of *Ihh* was also observed in *Wnt9a* mutant radii and ulnae (data not shown), but not in digits (see Fig. S2B,C in the supplementary material). This suggests that Wnt9a signaling temporally and spatially regulates *Ihh* in proximal long bones.

By contrast, the expression domain of the gene encoding parathyroid hormone receptor 1 (*Ppr*; *Pthr1* – Mouse Genome Informatics), which overlaps with *Ihh*, was reduced only in extent not in magnitude at E13.5 and E14.5, reflecting a delay in chondrocyte maturation (Fig. 5E; data not shown). The *collagen 10a1 (Col10a1)* expression domain, which marks hypertrophic chondrocytes, was slightly expanded in *Wnt9a* mutant humeri at E12.5 (Fig. 5F), while it was either reduced or not detectable at E13.5 (Fig. 5G; data not shown). At E14.5 the *Col10a1* domain in mutants resembled that of E13.5 wild-type humeri (Fig. 5H). This marker analysis showed that Wnt9a signaling is crucial for chondrocyte maturation around E12.5-E13.5.

Temporal downregulation of Ihh signaling in Wnt9a mutant long bones

Because *Ihh* expression was temporarily downregulated, we analyzed whether Ihh signaling and Ihh regulated processes were also affected. Analysis of the Ihh target genes patched 1 (*Ptch1*), which functions also as a receptor for Ihh, and *Pthrp* (St-Jacques et al., 1999; Vortkamp et al., 1996), showed a reduced expression in *Wnt9a*$^{-/-}$ humeri at E13.5 (Fig. 5I,J). Ihh signaling also regulates chondrocyte proliferation in a Pthrp-independent fashion (Karp et al., 2000). Consistent with the reduction in *Ihh* levels BrdU incorporation revealed a 7% reduction of the chondrocyte proliferation rate within the flattened zone at E13.5 ($P<0.05$; data

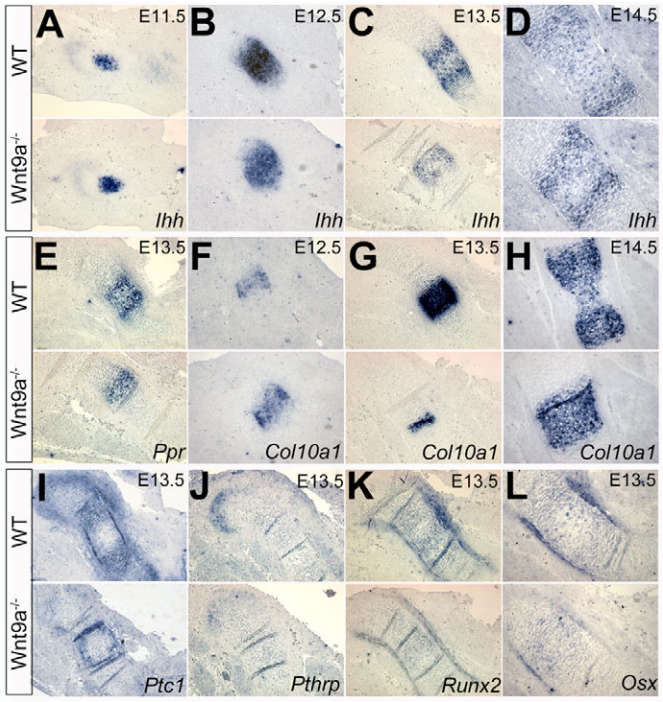

Fig. 5. Temporal regulation of *Ihh* expression by Wnt9a signaling. In situ hybridization on serial sections showing the humerus region of wild-type and *Wnt9a*$^{-/-}$ littermates. (**A-D**) Ihh expression at E11.5, E12.5, E13.5 and E14.5 in wild-type and Wnt9a$^{-/-}$; showing no significant difference at E11.5 (A), downregulation of *Ihh* expression at E12.5 (B) and E13.5 (C), and delayed separation of the *Ihh* expression domains at E14.5 (D) in *Wnt9a*$^{-/-}$ humeri. (**E**) Size reduction of the *Ppr* expression domain in *Wnt9a*$^{-/-}$ humeri compared with wild type at E13.5. (**F**) Increased *Col10a1* expression domain at E12.5 in *Wnt9a*$^{-/-}$ humeri. (**G**) Strongly reduced *Col10a1* expression domain at E13.5 and E14.5 (**H**) in *Wnt9a*$^{-/-}$ humeri. Reduced expression levels of *Ptch1* in chondrocytes and perichondrium (**I**), of *Pthrp* in the articular region (shoulder joint) (**J**), and of *Runx2* (**K**) and *Osx* (**L**) in the perichondrium/periosteum.

not shown). No significant difference in proliferation rate could be detected in mutant compared with wild-type humeri at E14.5 (data not shown).

Ihh plays a third role during endochondral bone formation; it is required for osteoblastogenesis in the perichondrium/periosteum (Long et al., 2004; St-Jacques et al., 1999). Analyses of various periosteal markers, such as *Runx2*, osterix (*Osx*; *Sp7* – Mouse Genome Informatics), osteopontin (*Op*; *Spp1* – Mouse Genome Informatics) and *Bmp3*, at E13.5 revealed that the expression of all four markers was reduced (Fig. 5K,L; data not shown). However, at E14.5, expression of these markers was comparable with wild type at E13.5 (data not shown). These data demonstrate that loss of Wnt9a activity results in a temporary reduction of Ihh signaling. This ultimately leads to a delay by ~1 day in chondrocyte and osteoblast maturation. Although *Ihh* levels are back to normal at around E14.5, the maturation delay cannot be compensated and thereby remains noticeable even at birth, reflected in the shortening of proximal skeletal elements.

Fgf signaling has also been shown to negatively regulate *Ihh* (Chen et al., 2001; Li et al., 1999; Minina et al., 2002; Naski et al., 1998). Therefore, we addressed whether Fgf signaling is involved in the temporary downregulation of *Ihh* in Wnt9a mutants by assaying for altered *Fgf* expression of 19 Fgf genes (Fgf1-13, Fgf15, 17, 18 and Fgf20-22) using real-time PCR at E12.5 and E13.5. With the exception of *Fgf4*, which was downregulated, none of the Fgf genes analyzed showed any significant increase or decrease in relative expression levels at E12.5 (see Fig. S3A in the supplementary material; data not shown). Interestingly at E13.5 the relative expression levels of five Fgf genes (*Fgf1*, *Fgf6*, *Fgf15*, *Fgf20* and *Fgf21*) were increased (see Fig. S3B in the supplementary material). This increase could potentially contribute to downregulation of *Ihh* at E13.5. To further investigate this possibility, we analyzed the expression of *Ihh* and *Col10a1* in humeri of embryos with constitutive active Fgfr3 signaling in chondrocytes (*Fgfr3ach* G380R) (Naski et al., 1998). However, no downregulation of *Ihh* expression was observed in humeri of *Fgfr3ach* mice at E12.5 (n=5) or E13.5 (n=10) (see Fig. S3C,D in the supplementary material). By contrast, we observed on average a slight expansion of the expression domains of *Ihh* (by ~8%) and *Col10* (by approx. 6%) at E13.5 compared with wild-type littermates (see Fig. S3D in the supplementary material). This suggests that activation of Fgfr3 signaling might promote chondrocyte maturation around E13.5.

As the upregulated Fgfs might not necessarily signal through Fgfr3, we performed limb explant cultures using E12.5 and E13.5 forelimbs from *Wnt9a* mutant, heterozygous and wild-type littermates to test whether inhibiting Fgf signaling in *Wnt9a* mutants would rescue *Ihh* expression levels. Limbs of corresponding limb pairs were cultured in the presence of DMSO or SU5402, a kinase inhibitor specific to Fgfrs (Mohammadi et al., 1997). Treatment with SU5402 resulted in a strong reduction in the domain size and expression levels of *Ihh* in wild-type and heterozygous E12.5 cultured humeri (n=5; see Fig. S3E in the supplementary material), while in E13.5 limbs only a size reduction was visible (see Fig. S4F in the supplementary material). In *Wnt9a*$^{-/-}$ E12.5 and E13.5 humeri, *Ihh* expression was even further downregulated (n=3; see Fig. S3E,F in the supplementary material). No *Col10a1* expression was detected at E12.5 in control and inhibitor-treated limbs (data not shown), while the *Col10a1* expression domain was not significantly affected at E13.5 (see Fig. S3G in the supplementary material). Treatment with SU5402 did not notably increase the size reduction of the *Col10a1* domain already present in *Wnt9a*$^{-/-}$ humeri, but as in the wild-type and heterozygous humeri, *Col10a1* expression was slightly decreased (see Fig. S3G in the supplementary material). Based on our analysis, we would conclude that Fgf signaling at early developmental stages is a positive regulator of chondrocyte maturation. Most importantly, our data suggest that Fgfs do not contribute to the observed downregulation of *Ihh* in *Wnt9a* mutants.

Wnt9a signals through β-catenin regulating chondrocyte maturation

Gain-of-function experiments suggested that Wnt9a signals through the canonical β-catenin pathway (Day et al., 2005; Guo et al., 2004) (this work). To assess this further, we looked at genetic interaction between *Wnt9a* and β-catenin with regard to chondrocyte maturation at E12.5-E15.5 in embryos double heterozygous for *Wnt9a* and β-catenin. At E12.5, but not at E13.5, *Ihh* expression levels were reduced in double-heterozygous embryos compared with wild-type or *Wnt9a*$^{+/-}$ littermates (Fig. 6A, and data not shown). Expression levels and domain size of *Ihh* were further reduced in *Wnt9a*$^{-/-}$;*β-cat*$^{+/-}$ in comparison with *Wnt9a*$^{-/-}$ single mutants at E12.5 (Fig. 6A). *Ptch1* expression in chondrocytes and periosteal cells at E13.5 was only slightly reduced in the double heterozygous humeri (Fig. 6A). In *Wnt9a*$^{-/-}$;*β-cat*$^{+/-}$ humeri, a further reduction in *Ptch1* expression in comparison with *Wnt9a* single mutants was

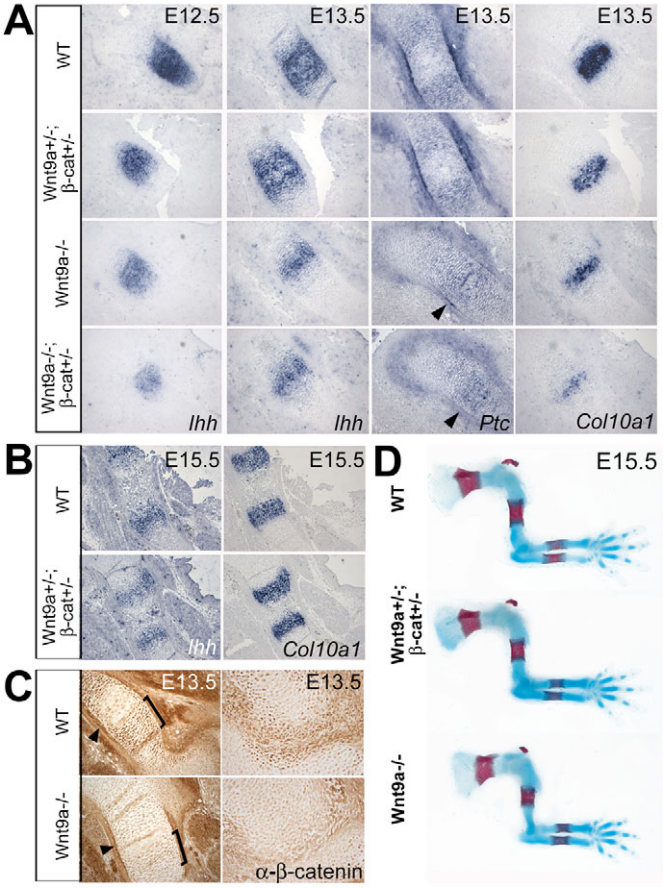

Fig. 6. Genetic interaction of *Wnt9a* and β-catenin in chondrocyte maturation. (**A**) In situ hybridization for *Ihh*, *Ptch1* and *Col10a1* on alternating sections of humeri from wild type, *Wnt9a*$^{+/-}$;*β-cat*$^{+/-}$, *Wnt9a*$^{-/-}$ and *Wnt9a*$^{-/-}$;*β-cat*$^{+/-}$ mutant littermates. Arrowheads indicate reduced expression of Ptch1. (**B**) In situ hybridization on E15.5 wild-type and *Wnt9a*$^{+/-}$;*β-cat*$^{+/-}$ humeri, showing that the *Ihh* and *Col10a1* expression domains are closer together in *Wnt9a*$^{+/-}$;*β-cat*$^{+/-}$ humeri compared with WT. (**C**) Immunohistochemical staining at E13.5, showing reduced β-catenin levels in flattened and prehypertrophic chondrocytes (bracket) in *Wnt9a* mutants in comparison with wild type above. Similar β-catenin levels are found in the periosteum (arrowheads). (**D**) Alcian Blue/Alizarin Red stained forelimbs of E15.5 wild type, *Wnt9a*$^{+/-}$;*β-cat*$^{+/-}$ and *Wnt9a*$^{-/-}$ embryos, showing a similar size reduction of the mineralized regions of scapula and humerus in double heterozygous mutants compared with *Wnt9a* single mutants.

primarily noticeable in the periosteum, where *Ptch1* was less strongly expressed (arrowheads in Fig. 6A). The *Col10a1* expression domain was also reduced in size in the double heterozygous at E13.5 and even further reduced in *Wnt9a*$^{-/-}$;*β-cat*$^{+/-}$ mutant humeri (Fig. 6A). At E15.5, the expression domains of *Ihh* and *Col10a1* were closer together in *Wnt9a*$^{+/-}$;*β-cat*$^{+/-}$ mutant humeri compared with wild type (Fig. 6B), demonstrating a delay in chondrocyte maturation. This delay in chondrocyte maturation and mineralization was also noticeable in skeletal preparations of E15.5 embryos, where the mineralized region in the long bones, particularly scapula and humerus, was reduced in size in *Wnt9a*$^{+/-}$;*β-cat*$^{+/-}$ to a similar extent as in *Wnt9a*$^{-/-}$ embryos (Fig. 6D). Consistent with the observation that Wnt9a signaling led to stabilization of β-catenin, nuclear β-catenin levels were reduced in prehypertrophic chondrocytes and in articular chondrocytes in *Wnt9a*$^{-/-}$ skeletal elements (Fig. 6C). Thus, Wnt9a is probably regulating chondrocyte maturation and *Ihh* expression through the canonical Wnt/β-catenin pathway.

Regulation of Ihh expression by β-catenin/Lef-1

Our data suggested that *Ihh* could be a direct target for the β-catenin/TCF-complex. This is supported by the presence of three potential TCF-binding sites within the *Ihh* promoter (Fig. 7A). Binding of a β-catenin/TCF-complex to the *Ihh* promoter was shown by in vivo chromatin immunopreciptation (ChIP) using cell lysates from E13.5 wild-type skeletal elements. Antibodies against β-catenin and Lef1 could immunoprecipitate three different regions of the *Ihh* promoter, each containing one of the potential binding sites (Fig. 7B). Performing ChIP assays with an antibody against H3K4 confirmed that the chromatin was in a transcriptionally active state. Real-time PCR analysis revealed that the TCF/Lef site closest to the putative transcriptional start site showed the strongest interaction with β-catenin and Lef1 (Fig. 7B). Therefore, we propose that the canonical Wnt pathway directly regulates *Ihh* transcription and that Wnt9a is the relevant ligand.

DISCUSSION

Wnt signaling is required to suppress the chondrogenic potential of joint cells

All joints are initially formed in *Wnt9a* mutants; however, loss of Wnt9a leads to ectopic differentiation of cartilage in the sagittal suture, to partial joint fusions of carpal and tarsal elements, and to synovial chondroid metaplasia in the HRJ. Double mutant analyses showed that Wnt9a and Wnt4 signaling is cooperatively required to suppress the chondrogenic potential of synovial and other joint cells in different types of joints. Nevertheless, not all joints are affected. This could be due to the presence of another Wnt gene, *Wnt16*. Our analysis suggests that Wnts might not be required for joint induction as previously proposed (Guo et al., 2004; Hartmann and Tabin, 2001). This is further supported by the observation that even the fusion of the three carpal elements (2, c and 3) present in *Wnt9a;Wnt4* double mutant newborns was not due to a defect in the initial joint formation. Both Wnts might use the β-catenin pathway (Guo et al., 2004; Hartmann and Tabin, 2000), therefore we examined the expression of joint markers during early stages of limb development in mice lacking β-catenin in the limb mesenchyme (Hill et al., 2005). This revealed that early joint interzone markers such as *Gdf5*, *Wnt4* and *Gli1* were still expressed in the presumptive joint regions at E11.5 (see Fig. S4 in the supplementary material), suggesting that canonical Wnt-signaling is not required for induction of those joint markers. However, as previously reported, their expression was lost and the joints never properly formed, resulting in partial fusions at later stages (Guo et al., 2004) (data not shown). Previous work has shown that synovial tissue contains chondroprogenitors (Nalin et al., 1995; Nishimura et al., 1999). Thus, it is likely that, analogous to its function in osteo-chondroprogenitors (Day et al., 2005; Hill et al., 2005), canonical Wnt/β-catenin signaling is required in an autocrine fashion to suppress the chondrogenic potential of cells in the presumptive joint region, thereby enabling joint formation and maintaining the integrity of the joint at later stages. Based on our analyses we would postulate that in the synovium and joint capsule there are still bi-potenial synovioprogenitors present at later stages of joint development, and that continuous canonical Wnt signaling is essential to suppress their chondrogenic potential thereby maintaining joint integrity. This strong pro-synovial anti-

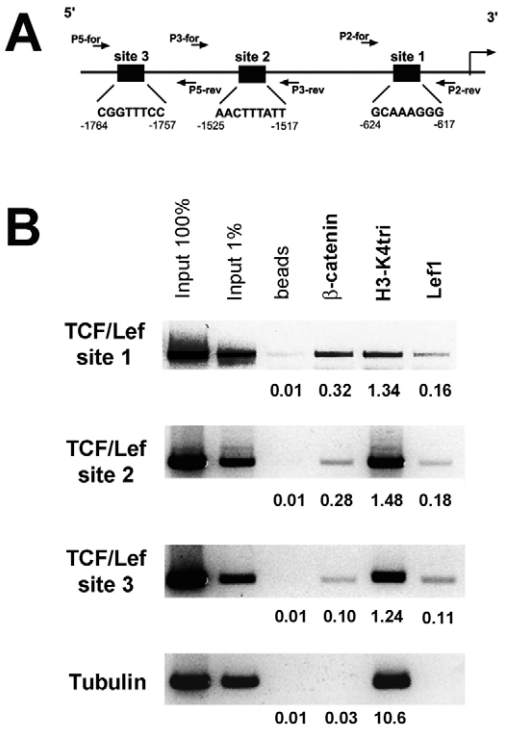

Fig. 7. β-Catenin and Lef1 physically interact with the *Ihh* promoter. (**A**) Schematic view of the 2.0 kb *Ihh* promoter region, showing the position of the three potential TCF/Lef1-binding sites relative to the translational start site (+1). (**B**) Chromatin immunoprecipitation for β-catenin, H3-K4 tri-methylation and Lef1 from E13.5 dissociated wild-type humeri, showing immunoprecipitation of all three sites in the *Ihh* promoter, but none of the *tubulin* promoter. Real-time PCR quantification (normalized to input and indicated by the numbers below) revealed that site 1 is bound with the highest affinity and site 3 with the lowest (n=3).

chondrogenic activity of canonical Wnt signaling on chondroprogenitors is also reflected in the ability of ectopic Wnt9a activity to transform chondrocytes into synoviofibroblast-like cells and to redirect early skeletal condensations to a joint fate (Guo et al., 2004; Hartmann and Tabin, 2000). However, this Wnt activity does not seem to be involved in normal joint induction.

Wnt9a a temporal regulator of Ihh controlling the size of skeletal elements

In addition, we discovered a role for Wnt9a signaling in chondrogenesis. Skeletal elements differ in size and shape; however, how this is regulated is largely unknown, but there is evidence that signals from the joint might be involved in the size regulation. One way to control size would be through modulation of Ihh signaling, a central regulator of endochondral bone formation (Kronenberg, 2003). Mutations affecting chondrocyte maturation or proliferation predominantly lead to size reduction of all or sometimes only individual skeletal elements. Here, we show that Wnt9a signaling temporally and spatially regulates *Ihh* expression in the appendicular skeleton. It is required around E12.5-E13.5 to maintain high levels of *Ihh* expression, but seems to be dispensable from E14.5 onwards. Temporary downregulation of *Ihh* results in reduced chondrocyte proliferation, and a delay of chondrocyte maturation and osteoblastogenesis by approximately 1 day and ultimately in shortening of the proximal long bones. *Fgf* signaling has also been implicated in negatively regulating *Ihh* expression and could potentially mediate the effect seen in *Wnt9a* mutants (Ornitz and Marie, 2002). However, *Ihh* expression was not downregulated in E12.5 and E13.5 limbs of *Fgfr3ach* mice and no significant increase in the expression levels of *Fgfs* was observed in *Wnt9a* mutants at E12.5. Our Fgf signaling analyses, instead, suggest that Fgfs might actually contribute to restoring normal chondrocyte maturation in *Wnt9a* mutants from E14.5 onwards, concomitant with an upregulation of some Fgfs. Thus, *Ihh* expression is probably negatively regulated by Wnt signaling and Fgf signaling at different developmental time points. Therefore, it is tempting to speculate that sequential signaling input through different pathways, converging on the regulation of *Ihh*, which is at the heart of the endochondral bone formation process, could be a crucial mechanism to control the size of individual appendicular skeletal elements.

Wnt9a regulates Ihh expression through the canonical β-catenin pathway

The levels of β-catenin are reduced in prehypertrophic chondrocytes in *Wnt9a* mutants, while *Wnt9a* overexpression leads to an increase of β-catenin in vitro. This, together with the fact that β-catenin and Lef1 associate with the *Ihh* promoter in vivo, suggests that Wnt9a-dependent regulation of *Ihh* is probably mediated via the canonical/β-catenin pathway. This is further supported by the observations that *Ihh* expression levels in humeri of *Wnt9a;*β-catenin double heterozygous animals were slightly reduced and that *Ihh* expression varies from downregulation to temporary loss or delayed expression in skeletal elements of mice lacking β-catenin activity depending on the Cre-deleter line (T.P.H. and C.H., unpublished) (Akiyama et al., 2004; Hu et al., 2005). *Ihh* expression in the humerus and femur is also transcriptionally dependent on *Runx2*, and in more distal bones it requires the activity of *Runx2* and *Runx3* (Inada et al., 1999; Kim et al., 1999; Yoshida et al., 2004). *Runx2* has been recently suggested to be direct target for canonical Wnt/β-catenin signaling in osteoblasts (Gaur et al., 2005); however, chondrogenic *Runx2* expression levels were not significantly changed at the onset of *Ihh* downregulation at E12.5 in *Wnt9a* mutants (data not shown). The slight decrease in *Runx2* levels at later stages is probably due to the downregulation of *Ihh*, as *Runx2* expression is dependent on Ihh signaling (Hu et al., 2005; Long et al., 2004). Furthermore, *Runx2* expression was also not significantly altered in β-catenin mutant limbs (Day et al., 2005; Hill et al., 2005; Hu et al., 2005). Interestingly, Runx2 activity in chondrocytes is modulated by interaction with co-repressors such as HDAC4 and co-activators such as groucho 5 (Vega et al., 2004; Wang et al., 2004). Groucho 5 (*Grg5*; *Aes* – Mouse Genome Informatics) acts as a de-repressor in β-catenin/TCF signaling, unlike groucho 1-4, which act as co-repressors (Brantjes et al., 2001). Intriguingly, *Grg5*$^{-/-}$ mice display a postnatal, temporary reduction in *Ihh* expression, which is further dependent on *Runx2* levels (Wang et al., 2004; Wang et al., 2002). Thus, it is conceivable that the β-catenin/Lef1 complex and Runx2 could cooperatively regulate *Ihh*. Our data, together with published observations, suggest that Wnt signaling regulates the level of *Ihh* expression temporally during embryonic and postnatal development, thereby controlling chondrocyte maturation and the growth of skeletal elements.

A Wnt canon controlling skeletogenesis

The fact that the effect of *Wnt9a* regulation is only temporary can be explained by the presence of other Wnt genes, which could potentially compensate at later stages for the loss of *Wnt9a* activity.

Interestingly, when we analyzed the expression levels of various Wnt genes (*Wnt4*, *Wnt5a*, *Wnt5b* and *Wnt6*) by semi-quantitative and real-time RT-PCR, we found that *Wnt4* expression was elevated at E12.5 and E13.5 in *Wnt9a* mutant compared with wild-type humeri (see Fig. S5C in the supplementary material; data not shown). Concomitantly, chondrocyte maturation was further delayed in *Wnt9a/Wnt4* double mutant humeri (see Fig. S5A in the supplementary material); however, this did not result in further reduction of *Ihh* expression levels. *Wnt4* has been suggested to be a positive regulator of chondrocyte maturation (Hartmann and Tabin, 2000). Although *Wnt4* mutant mice have no reported skeletal phenotype (Stark et al., 1994), we did observe a slight delay in chondrocyte maturation in the appendicular skeleton of single mutants (see Fig. S5B in the supplementary material). Our loss-of-function analysis, together with previous gain-of-function data (Guo et al., 2004; Hartmann and Tabin, 2000), suggests that both *Wnt9a* and *Wnt4* are positive regulators of chondrocyte maturation.

Therefore, we propose the following model for Wnts and chondrogenesis: *Wnt9a* signals from the perichondrium or joints and regulates *Ihh* levels, probably via the canonical pathway, thereby regulating the pace of chondrocyte proliferation and maturation. In addition, Wnt9a signaling seems to negatively control *Wnt4*, which is expressed in prehypertrophic chondrocytes from E12.5 onwards (see Fig. S5D in the supplementary material). Wnt4 signaling regulates chondrocyte maturation at the transition from prehypertrophic to hypertrophic chondrocytes, but does not alter *Ihh* levels. Similarly, Wnt5a, which is expressed in the perichondrium and prehypertrophic chondrocytes, controls chondrocyte proliferation and maturation independently of *Ihh* (Yang et al., 2003). Part of the *Wnt5a* loss-of-function phenotype might be due to attenuation of β-catenin-mediated activities (Topol et al., 2003). Surprisingly, the phenotypes of the *Wnt5a* loss- and gain-of-function mice are very similar (Yang et al., 2003). Therefore, it will be interesting to test whether those phenotypes depend in part on β-catenin.

In addition, our work shows that Wnt signaling is required to maintain joint integrity by actively suppressing chondrocyte differentiation. Interestingly, *Ihh* mutant mice also display joint defects (St-Jacques et al., 1999) and recent work has shown that the canonical Wnt pathway is affected in *Ihh* mutants (Hu et al., 2005). Pathological alterations of the joint with spontaneous formation of cartilaginous nodules are known in humans as synovial chondromatosis. The etiology of this disease is largely unknown. However, deregulation of hedgehog signaling has recently been implicated in disease predisposition (Hopyan et al., 2005). It originates from chondroid metaplasia of connective tissue of the synovial membrane, causing pain, joint dysfunction and ultimately joint destruction. Thus, it will be important to examine whether the canonical Wnt/β-catenin pathway is altered in affected individuals.

We thank Cliff Tabin, in whose laboratory this work was started, for his support and generosity. Furthermore, we thank John Seidman for BAC reagents and for the C1 ES cells, Walter Birchmeier and Malcom Logan for mouse strains, Andrea Vortkamp and Manuela Wülling for the Fgfr3ach embryos, and Gail Martin and Naomi Fukai for reagents. We also thank Christian Theussl for blastocyst injections of Wnt9aLacZ ES cells, and Erwin Wagner and Latifa Bakiri for critical comments on the manuscript. This work was supported by Boehringer Ingelheim and the NoE Cells into Organs (LSHM-CT-2003-504468).

References

Akiyama, H., Lyons, J. P., Mori-Akiyama, Y., Yang, X., Zhang, R., Zhang, Z., Deng, J. M., Taketo, M. M., Nakamura, T., Behringer, R. R. et al. (2004). Interactions between Sox9 and beta-catenin control chondrocyte differentiation. *Genes Dev.* **18**, 1072-1087.

Archer, C. W., Dowthwaite, G. P. and Francis-West, P. (2003). Development of synovial joints. *Birth Defects Res. C Embryo Today* **69**, 144-155.

Brantjes, H., Roose, J., van De Wetering, M. and Clevers, H. (2001). All Tcf HMG box transcription factors interact with Groucho-related co-repressors. *Nucleic Acids Res.* **29**, 1410-1419.

Brunet, L. J., McMahon, J. A., McMahon, A. P. and Harland, R. M. (1998). Noggin, cartilage morphogenesis, and joint formation in the mammalian skeleton. *Science* **280**, 1455-1457.

Capdevila, J. and Johnson, R. L. (1998). Endogenous and ectopic expression of noggin suggests a conserved mechanism for regulation of BMP function during limb and somite patterning. *Dev. Biol.* **197**, 205-217.

Chen, L., Li, C., Qiao, W., Xu, X. and Deng, C. (2001). A Ser(365)→Cys mutation of fibroblast growth factor receptor 3 in mouse downregulates Ihh/PTHrP signals and causes severe achondroplasia. *Hum. Mol. Genet.* **10**, 457-465.

Day, T. F., Guo, X., Garrett-Beal, L. and Yang, Y. (2005). Wnt/beta-catenin signaling in mesenchymal progenitors controls osteoblast and chondrocyte differentiation during vertebrate skeletogenesis. *Dev. Cell* **8**, 739-750.

Debeer, P., Huysmans, C., Van de Ven, W. J., Fryns, J. P. and Devriendt, K. (2005). Carpal and tarsal synostoses and transverse reduction defects of the toes in two brothers heterozygous for a double de novo NOGGIN mutation. *Am. J. Med. Genet. A* **134**, 318-320.

Francis-West, P. H., Richardson, M. K., Bell, E., Chen, P., Luyten, F., Adelfattah, A., Barlow, A. J., Brickell, P. M., Wolpert, L. and Archer, C. W. (1996). The effect of overexpression of BMPs and GDF-5 on the development of chick limb skeletal elements. *Ann. N. Y. Acad. Sci.* **785**, 254-255.

Francis-West, P. H., Parish, J., Lee, K. and Archer, C. W. (1999). BMP/GDF-signalling interactions during synovial joint development. *Cell Tissue Res.* **296**, 111-119.

Garciadiego-Cazares, D., Rosales, C., Katoh, M. and Chimal-Monroy, J. (2004). Coordination of chondrocyte differentiation and joint formation by alpha5beta1 integrin in the developing appendicular skeleton. *Development* **131**, 4735-4742.

Gaur, T., Lengner, C. J., Hovhannisyan, H., Bhat, R. A., Bodine, P. V., Komm, B. S., Javed, A., van Wijnen, A. J., Stein, J. L., Stein, G. S. et al. (2005). Canonical WNT signaling promotes osteogenesis by directly stimulating RUNX2 gene expression. *J. Biol. Chem.* **280**, 33132-33140.

Gong, Y., Krakow, D., Marcelino, J., Wilkin, D., Chitayat, D., Babul-Hirji, R., Hudgins, L., Cremers, C. W., Cremers, F. P., Brunner, H. G. et al. (1999). Heterozygous mutations in the gene encoding noggin affect human joint morphogenesis. *Nat. Genet.* **21**, 302-304.

Guo, X., Day, T. F., Jiang, X., Garrett-Beal, L., Topol, L. and Yang, Y. (2004). Wnt/beta-catenin signaling is sufficient and necessary for synovial joint formation. *Genes Dev.* **18**, 2404-2417.

Hartmann, C. and Tabin, C. J. (2000). Dual roles of Wnt signaling during chondrogenesis in the chicken limb. *Development* **127**, 3141-3159.

Hartmann, C. and Tabin, C. J. (2001). Wnt-14 plays a pivotal role in inducing synovial joint formation in the developing appendicular skeleton. *Cell* **104**, 341-351.

Hendrickson, B. A., Conner, D. A., Ladd, D. J., Kendall, D., Casanova, J. E., Corthesy, B., Max, E. E., Neutra, M. R., Seidman, C. E. and Seidman, J. G. (1995). Altered hepatic transport of immunoglobulin A in mice lacking the J chain. *J. Exp. Med.* **182**, 1905-1911.

Hill, T. P., Spaeter, D., Taketo, M. M., Birchmeier, W. and Hartmann, C. (2005). Canonical Wnt/beta-catenin signaling prevents osteoblasts from differentiating into chondrocytes. *Dev. Cell* **8**, 727-738.

Hopyan, S., Nadesan, P., Yu, C., Wunder, J. and Alman, B. A. (2005). Dysregulation of hedgehog signalling predisposes to synovial chondromatosis. *J. Pathol.* **206**, 143-150.

Hu, H., Hilton, M. J., Tu, X., Yu, K., Ornitz, D. M. and Long, F. (2005). Sequential roles of Hedgehog and Wnt signaling in osteoblast development. *Development* **132**, 49-60.

Huelsken, J., Vogel, R., Brinkmann, V., Erdmann, B., Birchmeier, C. and Birchmeier, W. (2000). Requirement for beta-catenin in anterior-posterior axis formation in mice. *J. Cell Biol.* **148**, 567-578.

Huelsken, J., Vogel, R., Erdmann, B., Cotsarelis, G. and Birchmeier, W. (2001). beta-Catenin controls hair follicle morphogenesis and stem cell differentiation in the skin. *Cell* **105**, 533-545.

Inada, M., Yasui, T., Nomura, S., Miyake, S., Deguchi, K., Himeno, M., Sato, M., Yamagiwa, H., Kimura, T., Yasui, N. et al. (1999). Maturational disturbance of chondrocytes in Cbfa1-deficient mice. *Dev. Dyn.* **214**, 279-290.

Karp, S. J., Schipani, E., St-Jacques, B., Hunzelman, J., Kronenberg, H. and McMahon, A. P. (2000). Indian hedgehog coordinates endochondral bone growth and morphogenesis via parathyroid hormone related-protein-dependent and -independent pathways. *Development* **127**, 543-548.

Kengaku, M., Capdevila, J., Rodriguez-Esteban, C., De La Pena, J., Johnson, R. L., Belmonte, J. C. and Tabin, C. J. (1998). Distinct WNT pathways regulating AER formation and dorsoventral polarity in the chick limb bud. *Science* **280**, 1274-1277.

Kim, I. S., Otto, F., Zabel, B. and Mundlos, S. (1999). Regulation of chondrocyte differentiation by Cbfa1. *Mech. Dev.* **80**, 159-170.
Koyama, E., Golden, E. B., Kirsch, T., Adams, S. L., Chandraratna, R. A., Michaille, J. J. and Pacifici, M. (1999). Retinoid signaling is required for chondrocyte maturation and endochondral bone formation during limb skeletogenesis. *Dev. Biol.* **208**, 375-391.
Kronenberg, H. M. (2003). Developmental regulation of the growth plate. *Nature* **423**, 332-336.
Li, C., Chen, L., Iwata, T., Kitagawa, M., Fu, X. Y. and Deng, C. X. (1999). A Lys644Glu substitution in fibroblast growth factor receptor 3 (FGFR3) causes dwarfism in mice by activation of STATs and ink4 cell cycle inhibitors. *Hum. Mol. Genet.* **8**, 35-44.
Long, F., Chung, U. I., Ohba, S., McMahon, J., Kronenberg, H. M. and McMahon, A. P. (2004). Ihh signaling is directly required for the osteoblast lineage in the endochondral skeleton. *Development* **131**, 1309-1318.
Martens, J. H., O'Sullivan, R. J., Braunschweig, U., Opravil, S., Radolf, M., Steinlein, P. and Jenuwein, T. (2005). The profile of repeat-associated histone lysine methylation states in the mouse epigenome. *EMBO J.* **24**, 800-812.
McLeod, M. J. (1980). Differential staining of cartilage and bone in whole mouse fetuses by alcian blue and alizarin red S. *Teratology* **22**, 299-301.
Merino, R., Macias, D., Ganan, Y., Economides, A. N., Wang, X., Wu, Q., Stahl, N., Sampath, K. T., Varona, P. and Hurle, J. M. (1999). Expression and function of Gdf-5 during digit skeletogenesis in the embryonic chick leg bud. *Dev. Biol.* **206**, 33-45.
Minina, E., Kreschel, C., Naski, M. C., Ornitz, D. M. and Vortkamp, A. (2002). Interaction of FGF, Ihh/Pthlh, and BMP signaling integrates chondrocyte proliferation and hypertrophic differentiation. *Dev. Cell* **3**, 439-449.
Mohammadi, M., McMahon, G., Sun, L., Tang, C., Hirth, P., Yeh, B. K., Hubbard, S. R. and Schlessinger, J. (1997). Structures of the tyrosine kinase domain of fibroblast growth factor receptor in complex with inhibitors. *Science* **276**, 955-960.
Nalin, A. M., Greenlee, T. K., Jr and Sandell, L. J. (1995). Collagen gene expression during development of avian synovial joints: transient expression of types II and XI collagen genes in the joint capsule. *Dev. Dyn.* **203**, 352-362.
Naski, M. C., Colvin, J. S., Coffin, J. D. and Ornitz, D. M. (1998). Repression of hedgehog signaling and BMP4 expression in growth plate cartilage by fibroblast growth factor receptor 3. *Development* **125**, 4977-4988.
Nishimura, K., Solchaga, L. A., Caplan, A. I., Yoo, J. U., Goldberg, V. M. and Johnstone, B. (1999). Chondroprogenitor cells of synovial tissue. *Arthritis Rheum.* **42**, 2631-2637.
Ohbayashi, N., Shibayama, M., Kurotaki, Y., Imanishi, M., Fujimori, T., Itoh, N. and Takada, S. (2002). FGF18 is required for normal cell proliferation and differentiation during osteogenesis and chondrogenesis. *Genes Dev.* **16**, 870-879.
Opperman, L. A. (2000). Cranial sutures as intramembranous bone growth sites. *Dev. Dyn.* **219**, 472-485.
Ornitz, D. M. and Marie, P. J. (2002). FGF signaling pathways in endochondral and intramembranous bone development and human genetic disease. *Genes Dev.* **16**, 1446-1465.
Pathi, S., Rutenberg, J. B., Johnson, R. L. and Vortkamp, A. (1999). Interaction of Ihh and BMP/Noggin signaling during cartilage differentiation. *Dev. Biol.* **209**, 239-253.
Pizette, S. and Niswander, L. (2000). BMPs are required at two steps of limb chondrogenesis: formation of prechondrogenic condensations and their differentiation into chondrocytes. *Dev. Biol.* **219**, 237-249.
Ralphs, J. R. and Benjamin, M. (1994). The joint capsule: structure, composition, ageing and disease. *J. Anat.* **184**, 503-509.
Rountree, R. B., Schoor, M., Chen, H., Marks, M. E., Harley, V., Mishina, Y. and Kingsley, D. M. (2004). BMP receptor signaling is required for postnatal maintenance of articular cartilage. *PLoS Biol.* **2**, e355.
Settle, S. H., Jr, Rountree, R. B., Sinha, A., Thacker, A., Higgins, K. and Kingsley, D. M. (2003). Multiple joint and skeletal patterning defects caused by single and double mutations in the mouse Gdf6 and Gdf5 genes. *Dev. Biol.* **254**, 116-130.
St-Jacques, B., Hammerschmidt, M. and McMahon, A. P. (1999). Indian hedgehog signaling regulates proliferation and differentiation of chondrocytes and is essential for bone formation. *Genes Dev.* **13**, 2072-2086.
Stark, K., Vainio, S., Vassileva, G. and McMahon, A. P. (1994). Epithelial transformation of metanephric mesenchyme in the developing kidney regulated by Wnt-4. *Nature* **372**, 679-683.
Storm, E. E. and Kingsley, D. M. (1996). Joint patterning defects caused by single and double mutations in members of the bone morphogenetic protein (BMP) family. *Development* **122**, 3969-3979.
Storm, E. E. and Kingsley, D. M. (1999). GDF5 coordinates bone and joint formation during digit development. *Dev. Biol.* **209**, 11-27.
Storm, E. E., Huynh, T. V., Copeland, N. G., Jenkins, N. A., Kingsley, D. M. and Lee, S. J. (1994). Limb alterations in brachypodism mice due to mutations in a new member of the TGF beta-superfamily. *Nature* **368**, 639-643.
Sun, X., Lewandoski, M., Meyers, E. N., Liu, Y. H., Maxson, R. E., Jr and Martin, G. R. (2000). Conditional inactivation of Fgf4 reveals complexity of signalling during limb bud development. *Nat. Genet.* **25**, 83-86.
Topol, L., Jiang, X., Choi, H., Garrett-Beal, L., Carolan, P. J. and Yang, Y. (2003). Wnt-5a inhibits the canonical Wnt pathway by promoting GSK-3-independent beta-catenin degradation. *J. Cell Biol.* **162**, 899-908.
Tsumaki, N., Nakase, T., Miyaji, T., Kakiuchi, M., Kimura, T., Ochi, T. and Yoshikawa, H. (2002). Bone morphogenetic protein signals are required for cartilage formation and differently regulate joint development during skeletogenesis. *J. Bone Miner. Res.* **17**, 898-906.
Vega, R. B., Matsuda, K., Oh, J., Barbosa, A. C., Yang, X., Meadows, E., McAnally, J., Pomajzl, C., Shelton, J. M., Richardson, J. A. et al. (2004). Histone deacetylase 4 controls chondrocyte hypertrophy during skeletogenesis. *Cell* **119**, 555-566.
Vortkamp, A., Lee, K., Lanske, B., Segre, G. V., Kronenberg, H. M. and Tabin, C. J. (1996). Regulation of rate of cartilage differentiation by Indian hedgehog and PTH-related protein. *Science* **273**, 613-622.
Wang, W. F., Wang, Y. G., Reginato, A. M., Plotkina, S., Gridley, T. and Olsen, B. R. (2002). Growth defect in Grg5 null mice is associated with reduced Ihh signaling in growth plates. *Dev. Dyn.* **224**, 79-89.
Wang, W., Wang, Y. G., Reginato, A. M., Glotzer, D. J., Fukai, N., Plotkina, S., Karsenty, G. and Olsen, B. R. (2004). Groucho homologue Grg5 interacts with the transcription factor Runx2-Cbfa1 and modulates its activity during postnatal growth in mice. *Dev. Biol.* **270**, 364-381.
Yang, Y., Topol, L., Lee, H. and Wu, J. (2003). Wnt5a and Wnt5b exhibit distinct activities in coordinating chondrocyte proliferation and differentiation. *Development* **130**, 1003-1015.
Yoshida, C. A., Yamamoto, H., Fujita, T., Furuichi, T., Ito, K., Inoue, K., Yamana, K., Zanma, A., Takada, K., Ito, Y. et al. (2004). Runx2 and Runx3 are essential for chondrocyte maturation, and Runx2 regulates limb growth through induction of Indian hedgehog. *Genes Dev.* **18**, 952-963.